Improved direct torque control of induction motors using adaptive observer and sliding mode control

DJILALI KOUCHIH, MOHAMED TADJINE and MOHAMED SEGHIR BOUCHERIT

This paper presents the synthesis of an adaptive observer which is used for the improvement of the direct torque control of induction motor drives. The observer detects stator flux components in two-phase stationary reference frame, rotor speed and stator resistance by measure of the stator terminal voltages and currents. The observer is adapted using a simple algorithm which does not imply a high computational load. Stability analysis based on Lyapunov theory is performed in order to guarantee the closed loop stability. Simulation tests under load disturbance and stator resistance variation are provided to evaluate the consistency and performance of the proposed control technique in the low and high speeds.

Key words: adaptive observer, direct torque control, induction motor, sensorless, sliding mode control

1. Introduction

Direct Torque Control (DTC) is currently known as the technique being mostly employed to control induction motors (IM). It requires accurate knowledge of the magnitude and the angular position of the controlled flux. The flux is conventionally obtained from the stator voltage model, using the measured stator voltages and currents [1-2]. This method uses open loop pure integration and suffers from the well known problems, especially at low speed operation mode [3].

Many researchers have been involved in designing of sensorless control of the IM. Most methods are essentially based on the Model Reference Adaptive System (MRAS) or on the reactive power based reference model [4-5]. The MRAS algorithm is very simple but its greatest drawback is the sensitivity to uncertainties in the motor parameters. Others methods, based on Extended Kalman Filter (EKF) or on the intelligent techniques (fuzzy logic and neural networks), have been used by many authors [6-11]. These methods imply a high computational load. In addition, the variable structure techniques are also used by many researchers [12-16].

D. Kouchih is with Electronic Department, University Saad Dahlab, B.P. 270, Blida, Algeria. E-mail: djkouchih@yahoo.fr. M. Tadjine and M.S. Boucherit are with Process Control Laboratory, Automatic Control Department, ENP, 10, Avenue Badi H., B.P. 182, Alger, Algeria. E-mails: tadjine@yahoo.fr, ms_boucherit@yahoo.fr.

Generally, the rotor speed estimation is affected by parameter variations, especially the stator resistance due to temperature, particularly at low speeds [17-18]. Therefore, to improve the estimation of the components of the stator flux, it's necessary to compensate this parameter variation in sensorless control by using an online adaptation of the stator resistance.

On the other hand and for the speed control, the parametric variation modifies the performances of the control system when we use regulator with fixed parameters. However, the performances will be degraded face to internal and external disturbances [19]. To offer control robustness, many strategies have been proposed in literature [20-24]. In this work, we are interested to the Sliding Mode Control (SMC). The SMC can offer many good properties [25]. The problem of undesirable chattering can be remedied by replacing the switching function by a smooth continuous function [26].

2. DTC strategy

2.1. Principles

The basic idea of the DTC is to choose the optimal vector voltage which produces the desired flux and torque. The stator flux is given by:

$$\underline{\Phi}_s = \underline{\Phi}_{s0} + \int_0^t \left(\underline{V}_s - R_s \underline{I}_s \right) dt. \tag{1}$$

If the stator resistance is ignored, the stator flux can be approximated:

$$\underline{\Phi}_s \approx \underline{\Phi}_{s0} + \int_0^t \underline{V}_s dt. \tag{2}$$

During one period of sampling T_e, the vector voltage applied to the machine remains constant, we can write:

$$\underline{\Phi}_s(k+1) \approx \underline{\Phi}_s(k) + \underline{V}_s T_e, \tag{3}$$

so the increment is

$$\Delta \underline{\Phi}_s \approx \underline{V}_s T_e. \tag{4}$$

Therefore, to increase the stator flux, we can apply a vector of voltage that is co-linear in its direction and vice-versa.

The electromagnetic torque produced by the IM can be expressed:

$$C_e = k_T \Phi_s \Phi_r \sin\gamma \tag{5}$$

where k_T is a constant [18]. The electromagnetic torque depends upon the effective value of the stator flux and rotor flux and their relative position γ. Actual torque and flux are compared with the reference values and control signals are produced.

The stator voltage is being obtained using the following equation:

$$\underline{V}s = \frac{2U_{dc}}{3}\left[S_a + S_b e^{j\frac{2\pi}{3}} + S_c e^{j\frac{4\pi}{3}}\right]$$ (6)

where U_{dc}, S_i $(i = a, b, c)$ are DC voltage and the signals of the gats of the inverter, respectively. The choice of the stator vector voltage depends on the desired variation for the module of stator flux, upon its rotation sense and the desired evolution for the torque. Through the components of stator flux indicated by the reference point (α, β) bound to the stator, we can decompose the space of stator flux into six sectors [12]. The block diagram of an induction motor based DTC strategy is drawn in figure 1. The structure of adaptive observer is presented in figure 2.
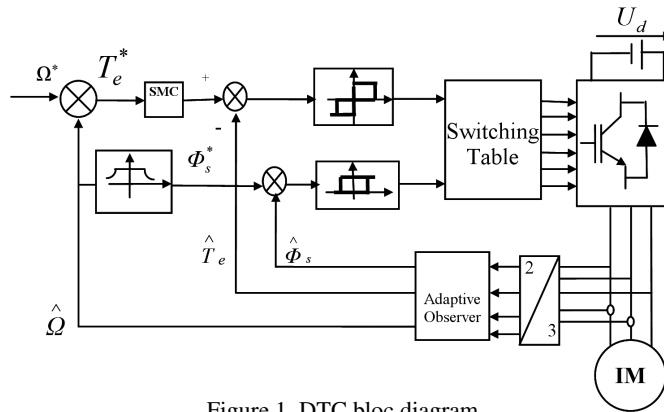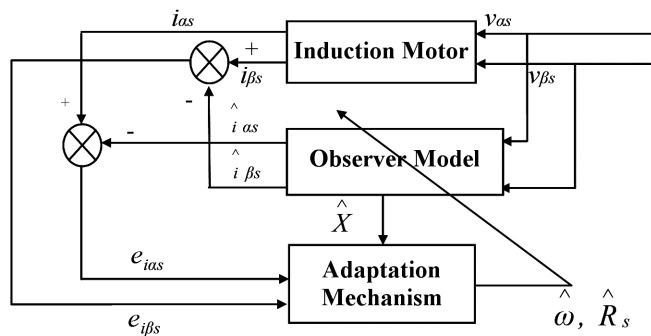

Figure 1. DTC bloc diagram.

Figure 2. Global adaptive observer.

2.2.   Correction of the stator flux

We use a two-level comparison of hysteresis in order to maintain the extremity of the vector of stator flux in one circular crown. A Boolean variable indicates if the amplitude of the flux must be increased ($\delta = 1$) or ($\delta = 0$) decreased in order to maintain:

$$|\Phi_s^* - \Phi_s| \leqslant \Delta\Phi_s \tag{7}$$

where Φ_s^* is the reference stator flux and $\Delta\Phi_s$ the stator flux hysteresis band.

2.3.   Correction of the torque

We use a three-level comparison of hysteresis in order to control the motor in both senses of rotation. Variable μ indicates if the torque must be increased ($\mu = 1$), to maintain its constant ($\mu = 0$) and ($\mu = -1$) to reduce the torque. This correction assures to operate in all four quadrants.

The stator voltage applied to the motor depends upon the position of the stator flux in the sectors. The optimal switching logic defines the best vector and flux references. Table 1 shows the switching order.

Table 5. Switching table of the IM based DTC

Sectors		1	2	3	4	5	6
$\delta = 1$	$\mu = +1$	110	010	011	001	101	100
	$\mu = 0$	111	000	111	000	111	000
	$\mu = -1$	101	100	110	010	011	001
$\delta = 0$	$\mu = +1$	010	011	001	101	100	110
	$\mu = 0$	000	111	000	111	000	111
	$\mu = -1$	001	101	100	110	010	011

2.4.   Correction of mechanical speed

To correct the mechanical speed, we use a sliding mode controller. The sliding mode technique is developed from variable structure control to reject the disturbances, modeling uncertainties or parameter variation. It is a technique to adjust feedback by previously defining surface [25]. The system which is controlled will be forced to that surface, then the behavior of the system slides to the desired equilibrium point.

Design of the control system will be demonstrated for a nonlinear multi-input system of the form [25]:

$$X_i^{(n_i)}(t) = f_i(X) + \sum_{j=1}^{m} b_{ij}(X)U_j, \quad i = 1,...,m, \quad j = 1,...,m \tag{8}$$

where the vector U of components U_j is the control input vector, and the state X is composed with X_i and their first $(n_i - 1)$ derivatives. Such systems are called square systems, since they have as many control inputs U_j as states to be controlled X_i. We are interested in the problem of having the state X track a desired time-varying state X^d.

Let us define a vector s of components s_i by:

$$s_i = \left(\frac{d}{dt} + \lambda_i\right)^{n_i-1} e_i, \tag{9}$$

$$e_i = X_i^d - X_i. \tag{10}$$

The purpose of the sliding mode control is to keep the system motion on the manifold S, which is defined as:

$$S = \{X : e = 0\} \tag{11}$$

where e is the tracking error vector

$$e = X^d - X. \tag{12}$$

The sliding mode control should be chosen such that the candidate Lyapunov function V_i satisfies the Lyapunov stability criteria. If we let:

$$V_i = \frac{1}{2}s_i^2 \tag{13}$$

then

$$\dot{V}_i = s_i \dot{s}_i. \tag{14}$$

The candidate Lyapunov function should satisfy the Lyapunov stability criteria. This can be assured for:

$$\frac{1}{2}\frac{d}{dt}s_i^2 = -\eta_i |s_i| \quad \eta_i > 0. \tag{15}$$

Equation (13) states that the squared distance to the surface, measured by s_i^2 decreases along all system trajectories. The control function can be expressed as follows [26]:

$$U_i^{com} = U_i^{eq} + U_i^{n} \tag{16}$$

Where U_i^{eq} is the equivalent control function and U_i^{n} is the correction factor which must be calculated so that the Lyapunov stability condition is satisfied. The correction factor can be expressed as [19]:

$$U_i^{n} = K_i \text{sgn}(s_i). \tag{17}$$

Here sgn is the sign function and K_i is the controller gain designed from the Lyapunov stability. It was well known that sliding mode technique generates undesirable chattering. This problem can be remedied by replacing the switching function by a smooth continuous function. One possible approximation is the sigmoid-like function [26]

$$sat(s_i) = \frac{s_i}{|s_i| + \psi_i} \tag{18}$$

where ψ_i is a small positive scalar.

For the correction of the mechanical speed, the control function will satisfy reaching conditions in the following form

$$T_e^* = T_e^{eq} + T_e^n \tag{19}$$

where T_e^* is the reference torque, T_e^{eq} is the equivalent control torque, T_e^n is the correction factor and must be calculated so that the stability condition for the selected control is satisfied.

For $n = 1$, the sliding surface can be expressed by:

$$s(\Omega) = \Omega^* - \Omega. \tag{20}$$

During the sliding mode and in permanent regime, we have:

$$s(\Omega) = 0, \quad \dot{s}(\Omega) = 0. \tag{21}$$

We have

$$\dot{\Omega} = \frac{1}{J}\left(Te - T_l - fv\Omega\right) \tag{22}$$

where J is the inertia of the rotor and the connected load, T_e the electromagnetic torque, T_l the load torque, Ω is the mechanical angular speed and f_v is the viscose friction coefficient. The equivalent control can be expressed as follows

$$T_e^{eq} = J\left(\dot{\Omega}^* + T_l + f_v\Omega\right). \tag{23}$$

During the convergence mode, the condition $s(\Omega)\dot{s}(\Omega) \leqslant 0$ must be verified. We obtain:

$$\dot{s}(\Omega) = -\frac{1}{J}T_e^n. \tag{24}$$

Therefore the correction factor is given by:

$$T_e^n = K \cdot sat\left(s\right). \tag{25}$$

To verify the system stability condition, parameter K must be positive.

3. Adaptive observer

The objective is to determine the adaptation mechanism of the speed and the stator resistance. The structure of the observer is based on the induction motor model in stator

reference frame. The state equations of the induction motor can be expressed as follows [27]:

$$
\begin{cases}
\dfrac{di_{\alpha s}}{dt} = -\dfrac{1}{\sigma L_s}\left(R_s + R_r\dfrac{L_m^2}{L_r^2}\right)i_{\alpha s} + \dfrac{1}{\sigma L_s}R_r\dfrac{L_m}{L_r^2}\Phi_{\alpha r} + \dfrac{1}{\sigma L_s}\omega\dfrac{L_m}{L_r}\Phi_{\beta r} + \dfrac{1}{\sigma L_s}v_{\alpha s} \\[2mm]
\dfrac{di_{\beta s}}{dt} = -\dfrac{1}{\sigma L_s}\left(R_s + R_r\dfrac{L_m^2}{L_r^2}\right)i_{\beta s} - \dfrac{1}{\sigma L_s}\omega\dfrac{L_m}{L_r}\Phi_{\alpha r} + \dfrac{1}{\sigma L_s}R_r\dfrac{L_m}{L_r^2}\Phi_{\beta r} + \dfrac{1}{\sigma L_s}v_{\beta s} \\[2mm]
\dfrac{d\Phi_{\alpha r}}{dt} = \dfrac{R_r L_m}{L_r}i_{\alpha s} - \dfrac{R_r}{L_r}\Phi_{\alpha r} - \omega\Phi_{\beta r} \\[2mm]
\dfrac{d\Phi_{\beta r}}{dt} = \dfrac{R_r L_m}{L_r}i_{\beta s} - \dfrac{R_r}{L_r}\Phi_{\beta r} + \omega\Phi_{\alpha r}
\end{cases}
\tag{26}
$$

where $v_{\alpha s}$, $v_{\beta s}$ are the components of stator voltage vector, i_{ds}, i_{qs} are the components of stator current vector, $\Phi_{\alpha r}$, $\Phi_{\beta r}$ are the components of rotor flux vector, σ is the leakage factor, R_s and R_r are stator and rotor resistance, L_s and L_r represent the stator and rotor cyclic inductances and L_m is the stator-rotor cyclic mutual inductance. ω is the mechanical pulsation.

The previous state system can be expressed in the form:

$$
\begin{cases}
\dfrac{dX}{dt} = AX + BU \\[2mm]
Y = CX
\end{cases}
\tag{27}
$$

where

$$
X^T = \begin{pmatrix} i_{\alpha s} & i_{\beta s} & \Phi_{\alpha r} & \Phi_{\beta r} \end{pmatrix}, \quad
Y = \begin{pmatrix} i_{\alpha s} \\ i_{\beta s} \end{pmatrix}, \quad
U = \begin{pmatrix} v_{\alpha s} \\ v_{\beta s} \end{pmatrix}.
$$

The matrices are defined by:

$$
A = \begin{pmatrix}
-a & 0 & \dfrac{R_r L_m}{L_r b} & \omega\dfrac{L_m}{b} \\[3mm]
0 & -a & -\omega\dfrac{L_m}{b} & \dfrac{R_r L_m}{L_r b} \\[3mm]
\dfrac{R_r L_m}{L_r} & 0 & -\dfrac{R_r}{L_r} & -\omega \\[3mm]
0 & \dfrac{R_r L_m}{L_r} & +\omega & -\dfrac{R_r}{L_r}
\end{pmatrix}
$$

$$
B = \begin{pmatrix}
\dfrac{1}{\sigma L_s} & 0 \\[3mm]
0 & \dfrac{1}{\sigma L_s} \\[3mm]
0 & 0 \\[2mm]
0 & 0
\end{pmatrix}, \quad
C = \begin{pmatrix}
1 & 0 & 0 & 0 \\
0 & 1 & 0 & 0
\end{pmatrix},
$$

$$a = \frac{1}{\sigma L_s}\left(R_s + R_r\frac{L_m^2}{L_r^2}\right), \quad b = \sigma L_s L_r, \quad \sigma = 1 - \frac{L_m^2}{L_s L_r}$$

A linear state observer can be then derived by considering the mechanical speed as a constant parameter since its variation is very slow in comparison to the electrical variables. The model of the observer is defined as follows [28]:

$$\begin{cases} \dfrac{d\hat{X}}{dt} = \hat{A}\hat{X} + BU + G\left(\hat{Y} - Y\right) \\ \hat{Y} = C\hat{X}. \end{cases} \tag{28}$$

The machine parameters are assumed to be perfectly known, the mechanical pulsation and the stator resistance are unknown. Let define:

$$\begin{aligned} \delta\omega &= \hat{\omega} - \omega \\ \delta R_s &= \hat{R}_s - R_s. \end{aligned} \tag{29}$$

The symbol „^" denotes estimated values and G is the observer gain matrix.

We will determine the differential system describing the evolution of the error:

$$e = X - \hat{X}. \tag{30}$$

The state matrix of the observer can be written as:

$$\hat{A} = A + \delta A \tag{31}$$

where

$$\delta A = \begin{pmatrix} -\dfrac{1}{\sigma L_s}\delta R_s & 0 & 0 & \dfrac{L_m}{b}\delta\omega \\ 0 & -\dfrac{1}{\sigma L_s}\delta R_s & -\dfrac{L_m}{b}\delta\omega & 0 \\ 0 & 0 & 0 & -\delta\omega \\ 0 & 0 & +\delta\omega & 0 \end{pmatrix}. \tag{32}$$

Then, we can write:

$$\frac{d\hat{X}}{dt} = \hat{A}\hat{X} + BU + G\left(\hat{Y} - Y\right) \tag{33}$$

or

$$\frac{d\hat{X}}{dt} = \hat{A}\hat{X} + BU + GCe. \tag{34}$$

From (27), (28) and (30), we get:

$$\frac{de}{dt} = AX - \hat{A}\hat{X} + GCe, \tag{35}$$

thus

$$\frac{de}{dt} = (A + GC)e - \delta A\hat{X}. \tag{36}$$

Let define the Lyapunov function as:

$$V = e^T e + \frac{(\delta\omega)^2}{\lambda_1} + \frac{(\delta R_s)^2}{\lambda_2} \tag{37}$$

where λ_1 and λ_2 are positive scalars. This function should contain terms of the differences $\delta\omega$ and δR_s to obtain mechanism adaptation.

The stability of the observer is guaranteed for the condition [25]:

$$\frac{dV}{dt} < 0. \tag{38}$$

The derivative of the Lyapunov function is as follows

$$\frac{dV}{dt} = 2e^T \frac{de}{dt} + 2\frac{\delta\omega}{\lambda_1}\frac{d\delta\omega}{dt} + 2\frac{\delta R_s}{\lambda_2}\frac{d\delta R_s}{dt}. \tag{39}$$

First element of (39) can easily calculated

$$2e^T \frac{de}{dt} = 2e^T (A + GC)e - 2e^T \delta A\hat{X}. \tag{40}$$

The rotor flux components can not be measured. The flux dynamic is faster than the machine parameters dynamic. Therefore, to simplify (40), we can accept that

$$\begin{aligned} \hat{\Phi}_{\alpha r} &= \Phi_{\alpha r} \\ \hat{\Phi}_{\beta r} &= \Phi_{\beta r}. \end{aligned} \tag{41}$$

Thus

$$e^T \delta A\hat{X} = \frac{L_m}{b}\delta\omega\left(\hat{\Phi}_{\beta r}e_{i\alpha s} - \hat{\Phi}_{\alpha r}e_{i\beta s}\right) - \frac{1}{\sigma Ls}\delta R_s\left(\hat{i}_{\alpha s}e_{i\alpha s} + \hat{i}_{\beta s}e_{i\beta s}\right). \tag{42}$$

For the second and third terms of (39), we can write

$$\begin{aligned} 2\frac{\delta\omega}{\lambda}\frac{d\delta\omega}{dt} &= 2\frac{\delta\omega}{\lambda_1}\frac{d}{dt}\hat{\omega} - 2\frac{\delta\omega}{\lambda_1}\frac{d}{dt}\omega \\ 2\frac{\delta R_s}{\lambda_2}\frac{d\delta R_s}{dt} &= 2\frac{\delta R_s}{\lambda_2}\frac{d}{dt}\hat{R}_s - 2\frac{\delta R_s}{\lambda_2}\frac{d}{dt}R_s. \end{aligned} \tag{43}$$

We consider the hypothesis of a slowly varying regime for the machine parameters, thus:

$$\begin{aligned} \frac{d\omega}{dt} &\approx 0 \\ \frac{dR_s}{dt} &\approx 0, \end{aligned} \tag{44}$$

thus

$$\frac{d\hat{\omega}}{dt} = \frac{d\delta\omega}{dt}$$

$$\frac{d\hat{R}_s}{dt} = \frac{d\delta R_s}{dt}. \tag{45}$$

Finally, we obtain:

$$
\begin{aligned}
\frac{dV}{dt} ={} & 2e^T(A+GC)e - \frac{2L_m}{b}\delta\omega\left(\hat{\Phi}_{\beta r}e_{i\alpha s} - \hat{\Phi}_{\alpha r}e_{i\beta s}\right) \\
& + \frac{2}{\sigma L_s}\delta R_s\left(\hat{i}_{\alpha s}e_{i\alpha s} + \hat{i}_{\beta s}e_{i\beta s}\right) + 2\frac{\delta\omega}{\lambda_1}\frac{d}{dt}\hat{\omega} + 2\frac{\delta R_s}{\lambda_2}\frac{d}{dt}\hat{R}_s.
\end{aligned}
\tag{46}
$$

If the term $\frac{dV}{dt} = 2e^T(A+GC)e$ is negative, the condition $\frac{dV}{dt} < 0$ is verified for:

$$
\begin{aligned}
& \frac{2}{\sigma L_s}\delta R_s\left(\hat{i}_{\alpha s}e_{i\alpha s} + \hat{i}_{\beta s}e_{i\beta s}\right) - \frac{2L_m}{b}\delta\omega\left(\hat{\Phi}_{\beta r}e_{i\alpha s} - \hat{\Phi}_{\alpha r}e_{i\beta s}\right) \\
& \qquad\qquad\qquad\qquad + 2\frac{\delta\omega}{\lambda_1}\frac{d}{dt}\hat{\omega} + 2\frac{\delta R_s}{\lambda_2}\frac{d}{dt}\hat{R}_s = 0.
\end{aligned}
\tag{47}
$$

This condition can be verified if:

$$
\begin{cases}
2\dfrac{\delta\omega}{\lambda_1}\dfrac{d}{dt}\hat{\omega} = \dfrac{2L_m}{b}\delta\omega\left(\hat{\Phi}_{\beta r}e_{i\alpha s} - \hat{\Phi}_{\alpha r}e_{i\beta s}\right) \\[2mm]
2\dfrac{\delta R_s}{\lambda_2}\dfrac{d}{dt}\hat{R}_s = -\dfrac{2}{\sigma L_s}\delta R_s\left(\hat{i}_{\alpha s}e_{i\alpha s} + \hat{i}_{\beta s}e_{i\beta s}\right).
\end{cases}
\tag{48}
$$

We obtain the adaptation mechanism in the form:

$$
\begin{cases}
\hat{\omega} = \displaystyle\int \lambda_1\dfrac{L_m}{b}\left(\hat{\Phi}_{\beta r}e_{i\alpha s} - \hat{\Phi}_{\alpha r}e_{i\beta s}\right)dt \\[2mm]
\hat{R}_s = \displaystyle\int -\lambda_2\dfrac{1}{\sigma L_s}\left(\hat{i}_{\alpha s}e_{i\alpha s} + \hat{i}_{\beta s}e_{i\beta s}\right)dt.
\end{cases}
\tag{49}
$$

The matrix of gain G is selected such as the eigenvalues of the matrix $A+GC$ are in the left plane half of the complex plan and that the real part of the eigenvalues is larger in absolute value than the real part of the eigenvalues of the state matrix A [28].

The estimated electromagnetic torque is expressed as: We obtain the adaptation mechanism in the form:

$$\hat{C}_e = \frac{3}{2}p\frac{L_m}{L_r}\left(\hat{\Phi}_{\alpha r}\hat{i}_{\beta s} - \hat{\Phi}_{\beta r}\hat{i}_{\alpha s}\right). \tag{50}$$

The reference of the stator flux Φ_{sn} is deduced using the equation of the induction motor steady-state model.

$$V_{sn} = \Phi_{sn}\frac{R_s}{L_s}\sqrt{\frac{\left(1 - \sigma\frac{L_sL_r}{R_sR_r}\omega_{sl}\omega_s\right)^2 + \left(\frac{L_r}{R_r}\omega_{sl} + \frac{L_s}{R_s}\omega_s\right)^2}{1 + \left(\frac{\sigma\omega_{sl}L_r}{R_r}\right)^2}} \tag{51}$$

where ω_{sl} is the rotor variables pulsation in nominal mode and V_{sn} is the nominal value of the stator phase voltage.

4. Simulation results

The technique presented in the previous sections, has been implemented in the MATLAB environment. The IM parameters has been as follows: 3 [kW], 220/380 [V], 50 [Hz], $R_s = R_r = 1.84[\Omega]$, $L_s = L_r = 0.17$ [H], $L_m = 0.16$ [H], $J = 0.0145$ [kgm^2], $f_v = 0.0038$ [Nms/rd].

4.1. Low speeds

To illustrate performances of the proposed control, we simulated a load-less starting up mode and nominal torque applied at time $t = 0.3$ [sec]. The synthesized observer allows us to reconstruct all the state variables. For the DTC simulation, torque and flux hysteresis bands are 0.2 [Nm] and 0.01 [Wb] respectively. The load torque is fixed to 20 [Nm]. The speed of reference equals to ±50 [rpm]. Figures 3-8 summarizes the control system performance.
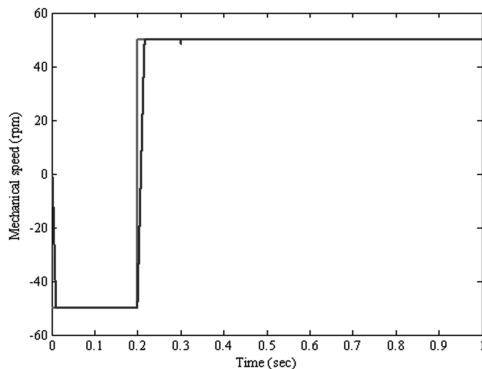
Figure 3. Observed and reference rotor speed.
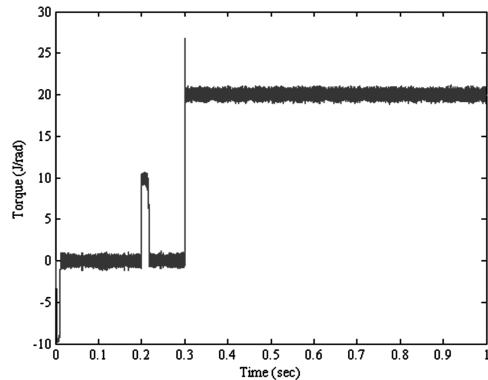
Figure 4. Observed electromagnetic torque.

4.2. High speed mode

The high speed mode depends on the machine and load mechanical possibilities. The load torque is an important factor for the choice of the acceptable high speed. The high speed mode is important, particularly in the case of electrical vehicles, wherein, we adopt the weakening of stator flux – see figure 9.

We simulated a load-less starting up mode with a speed of reference equals to 1415 [rpm]. Then at $t = 0.5$ [sec], we imposed a high speed of 2000 [rpm]. The simulation results are shown in figures 10-12.
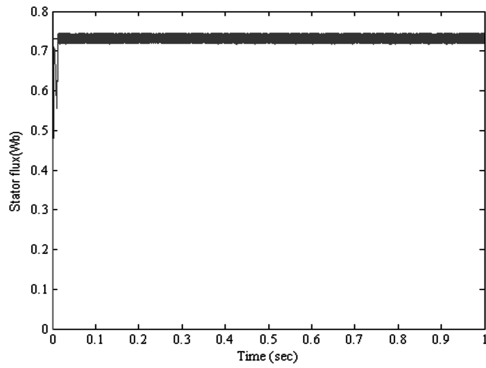
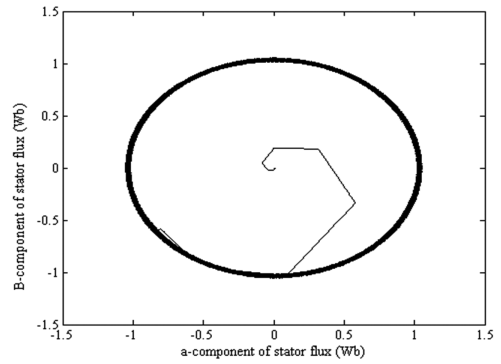Figure 5. Effective value of the stator flux.

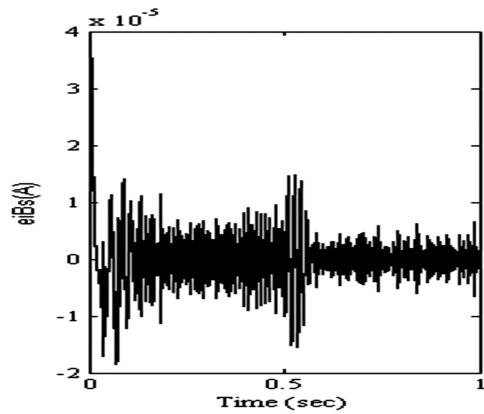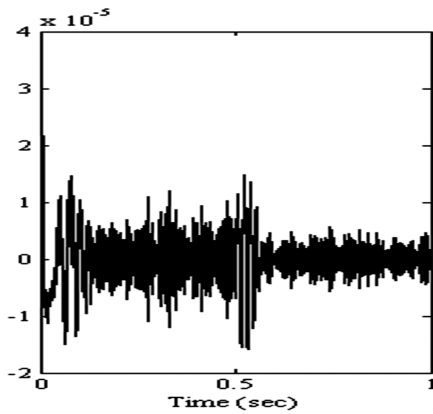
Figure 6. The hodograph of the stator flux vector.

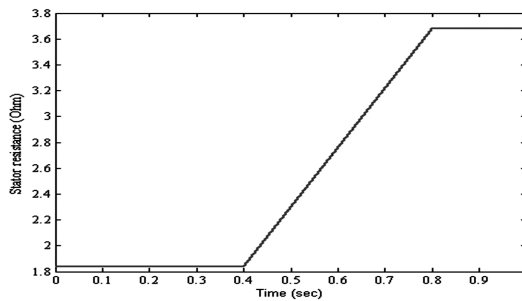Figure 7. Direct and quadrature stator currents errors.

Figure 8. Observed stator resistance.

From the simulation results, we can estimate the machine variables in the different working from low to high speeds. It appears that the load torque and stator resistance variations do not allocate the performances of the proposed control. The flux tracks the reference value and it is insensitive to parameters variation. The speed response also
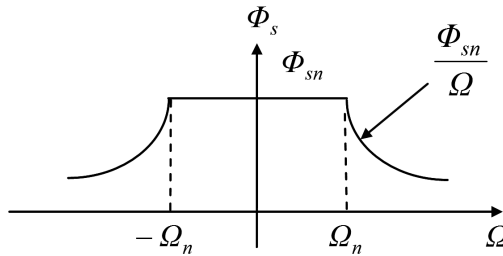
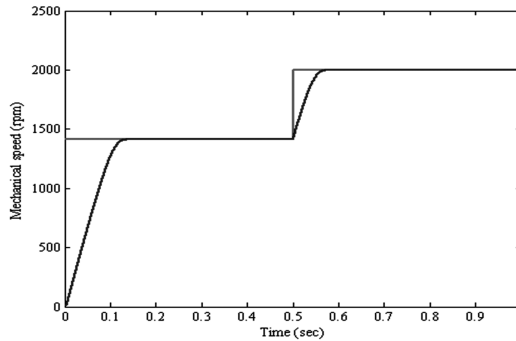Figure 9. Reference stator flux.

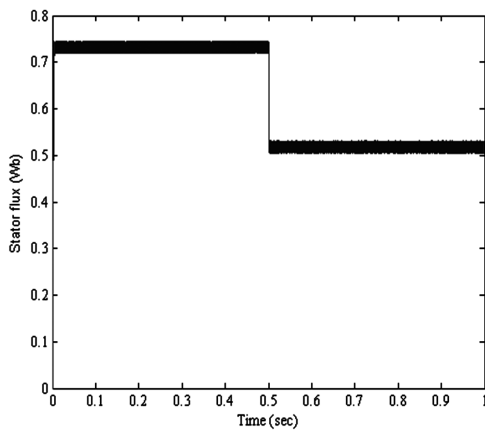Figure 10. Observed and referenced rotor speed.
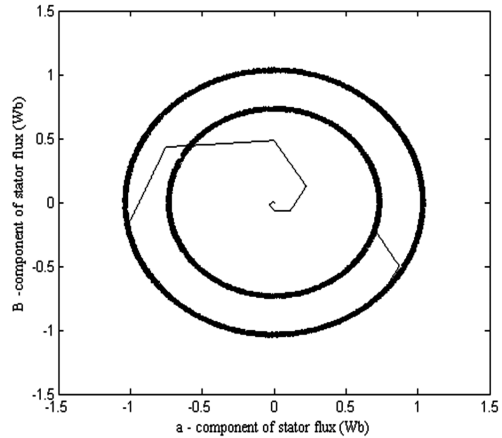

Figure 11. Effective value of the stator.

Figure 12. The hodograph of the stator flux vector.

stays insensitive to parameters variation. The global control scheme introduces high per-
formances of robustness, stability and precision, particularly, under uncertainties caused
by parameter variation.

5. Conclusion

In this paper a new adaptive observer design method has been presented. The global control scheme introduces high performances of robustness. Stability and precision, particularly, under uncertainties caused by load and stator resistance variation is also preserved. Furthermore, this observation method presents a simple algorithm that has the advantage to be easily implementable.

The adaptive observer uses an adaptive mechanism for the speed and the stator resistance estimation. This approach relies on the improvement of an estimation of the components of the stator flux.

We can note that the estimation of the stator flux by the adaptive observer makes the IM based on DTC more robust if stability is concerned.

References

[1] I. TAKAHASHI and T. NOGUCHI: A new quick-response and high-efficiency control strategy for an induction motor. *IEEE Trans. on Industry Applications*, **22**(5), (1986), 820-827.

[2] M. DEPENBROCK: Direct self-control DSC of inverter fed induction machine. *IEEE Trans. on Power Electronics*, **3**(4), (1988), 420-429.

[3] S. BELKACEM, F. NACERI, R. ABDESSEMED and B. KIYYOUR: Performance analysis of a speed sensorless induction motor drive based on DTC Scheme. *Int. J. of Electrical and Power Engineering*, **1**(2), (2007), 158-164.

[4] M. MESSAOUDI, H. KRAIM, M.B. AHMED, L. SBITA and M.N. ABDELKRIM: A robust sensorless direct torque control of induction motor based on MRAS and extended Kalman filter. *Leonardo J. of Sciences*, **12**(1), (2008), 35-56.

[5] K. SEDHURAMAN, S. HIMAVATHI and A. MUTHURAMALINGAM: Reactive power based model reference neural learning adaptive system for speed estimation in sensor-less induction motor drives. *The J. of Engineering Research*, **9**(2), (2011), 17-26.

[6] S. ALIRANI and V. JAGANNATHAN: Torque ripple minimization DTC based induction motor drive using fuzzy logic technique. *Int. J. of Computing Applications*, **40**(1), (2012), 25-31.

[7] M. AKTAS and H.I. OKUMUS: Stator resistance estimation using ANN in DTC IM Drives. *Turkish J. of Electrical Engineering and Computer Sciences*, **18**(2), (2010), 197-210.

[8] N. ALEKYA and B. MOHAN: Advanced technique to improve dynamic response of a direct torque controlled induction motor. *Int. J. of Scientific and Research Publications*, **2**(11), (2012), 1-6.

[9] H. KRAIEM, A. FLAH, M.B. HAMED and L. SBITA: High performances induction motor drive based on fuzzy logic control. *Int. J. of Control and Automation*, **5**(1), (2012), 1-11.

[10] Y. BENSALEM, W. ABBOUD, L. SBITA and M.N. ABDELKRIM: A sensorless neural network, Speed control of induction motor drive. *Int. J. of Signal System Control and Engineering Application*, **1**(2), (2008), 150-158.

[11] M.H. KHAN, A. AZAM and J. AMARNATH: Fuzzy logic based MRAS speed observer for control of induction motor drive. *World J. of Modelling and Simulation*, **6**(2), (2010), 134-140.

[12] S. ABID, Y. RAMDANI and A.K. MEROFEL: Speed sliding mode control of sensorless induction machine. *J. of Electrical Engineering*, **57**(1), (2006), 47-51.

[13] O. BARAMBONES, P. ALKORTA, A.J. GARRIDO and F.G. MESEDA: An adaptive sliding mode control scheme for induction motor drives. *Int. J. of Circuits, Systems and Signal Processing*, **1**(1), (2007), 73-77.

[14] W. SANGTUNGTONG: On improvement in the adaptive sliding-mode speed observer. *WSEAS Trans. on Systems*, **9**(6), (2010), 581-593.

[15] P.Y. REDDY, C.H. KRISHNA and P.V. KISHORE: A new approach of DTC scheme for induction motor using flux mode observer. *Int. J. of Engineering Research and Applications*, **1**(4), (2011), 1527-1535.

[16] X.Z. ZHANG and L. LI: A novel nonlinear controller design for induction motor drives based on sliding mode control and adaptive observer. *J. of Electrical Systems*, **7**(4), (2011), 382-393.

[17] B. TABBACHE, M.E.H BENBOUZID, A. KHELOUI and J.M. BOURGEOT: DSP based sensor fault tolerant control of electric vehicle powertrains. In *Proc. of the 2011 IEEE Int. Symp. on Industrial Electronics*, Gdansk, Poland, (2011), 2085-2090.

[18] A. ABBOU and H. MAHMOUDI: Performance of a sensorless direct torque flux control strategy for induction motors associated to the three levels NPC converter used in electric vehicles *Int. J. of Sciences and Techniques of Automatic Control & Computer Engineering*, **2**(2), (2008), 790-803.

[19] D. KOUCHIH, M. TADJINE and M.S. BOUCHERIT: Analysis of controlled induction motor drives with stator faults. In *Proc. of Int. Symp. on Environment Friendly*

Energies and Applications, Northumbria University, Newcastle upon Tyne, United Kingdom, (2012), 1-6.

[20] X. ZHANG and Y. WANG: Wavelet-neural-network based robust sliding-mode control for induction motor. *J. of Information & Computational Science*, **8**(7), (2011), 1209-1216.

[21] I.F. JASIM: Stable robust adaptive control of induction motors with unknown parameters. In *Proc. of the 1st Int. Conf. on Energy, Power and Control*, University of Baarah, Iraq, (2010), 145-150.

[22] Y.H. CHANG, C.I. WU, H.Y. LIN and N.D. KUO: Robust performance control of vector-controlled induction motors with gain scheduled estimation and input-output linearization. *Int. J. of Innovative Computing, Information and Control*, **7**(1), (2011), 269-288.

[23] O. BENZINEB, H. SALHI, M. TADJINE, M.S. BOUCHERIT and M.E.H BEN-BOUZID: A PI/backstepping approach for induction motor drives robust control. *Int. Review of Electrical Engineering*, **5**(2), (2010), 426-432.

[24] J.H. PUJAR and S.F. KODAD: Robust sensorless speed control of induction motor with DTFC and fuzzy speed regulator. *Int. J. of Electrical and Electronics Engineering*, **5**(1), (2011), 17-26.

[25] J.J.E. SLOTINE and W. LI: Applied Nonlinear Control. Prentice Hall Inc., Englewood Cliffs NJ, 1991.

[26] C. EDWARDS and S.K. SPURGEON: Sliding Mode Control, Theory and Applications. The Taylor & Francis Systems and Control Book Series, 1998.

[27] P.C. KRAUSE: Analysis of Electric Machinery. McGraw-Hill Book Company, 1987.

[28] D.G. LUENBERGER: An introduction to observers. *IEEE Trans. on Automatic Control*, **16**(6), (1971), 596-602.